SUPPORTING INFORMATION

Electronic Effects in Early Transition Metal Catalyzed Olefin Polymerization: Challenges in Featurization and Descriptor Strengths and Weaknesses.

Christian Ehm,[a,*] Gianluigi Galasso,[b] Antonio Vittoria,[a] Pietro Oriente,[a] Luigi Maiale,[a] Peter H.M. Budzelaar,[a] Roberta Cipullo[a] and Vincenzo Busico[a]

[a] Dipartimento di Scienze Chimiche, Università di Napoli Federico II, Via Cintia, 80126 Napoli, Italy;

[b] Scuola Superiore Meridionale, Via Mezzocannone 4, 80138 Napoli, Italy

*E-mail: christian.ehm@unina.it

Table of Contents

1. General comments 3

2. Descriptor evaluation and collection 5

3. Correlation between different model structures 7

4. Descriptors clustering analysis 9

5. Python scripts 20

6. References 23

1. General comments

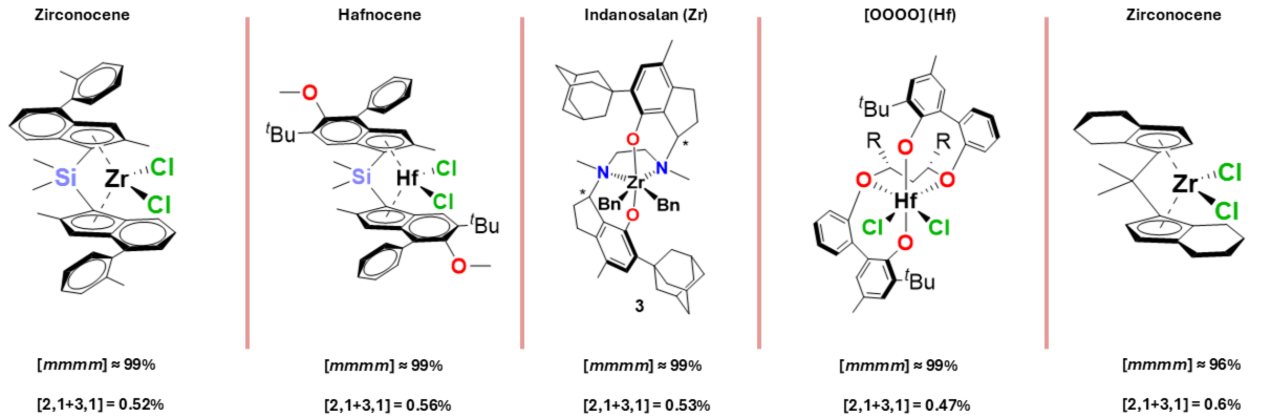

Figure S1. Different ligand/metal combinations yielding polymers with similar properties. From left to right: $SiMe_2$-bridged Zirconocene,[1] $SiMe_2$-bridged Hafnonocene,[1] Zr-based Indanosalan,[2] Hf-based [OOOO],[3] CMe_2-bridged Zirconocene.[4]

Table S1. Geometries of the different model structures for the various metal/ligand combinations studied.

Model structure	Sc	Y	Group 4
		***ansa*-metallocene**	
$LMCl_x$	trigonal	trigonal	tetrahedral
$LMMe_x$	distorted tetrahedral	distorted tetrahedral	tetrahedral
ACM	tetrahedral / in-plane	tetrahedral / in-plane	tetrahedral / in-plane
TSM	tetrahedral / in-plane	tetrahedral / in-plane	tetrahedral / in-plane
		Phosphinimide	
$LMCl_x$	trigonal	trigonal	tetrahedral
$LMMe_x$	trigonal	trigonal	tetrahedral
ACM	tetrahedral / out-of-plane	tetrahedral / in-plane	tetrahedral / out-of-plane
TSM	tetrahedral / in-plane	tetrahedral / in-plane	tetrahedral / in-plane
		Kol-type Salan	
$LMCl_x$	fac-fac	fac-mer	fac-fac
$LMMe_x$	tbp	fac-mer	fac-fac
ACM	fac-fac / in-plane	fac-mer / in-plane	fac-fac / in-plane
TSM	fac-fac / in-plane	fac-fac / in-plane	fac-fac / in-plane

The raw data for all the descriptors collected for this work are available in the "Raw_data.xlsx" file. The coding for the atoms of the ACM and TSM employed in the file, as well as in this document, is depicted in **Figure S2**.

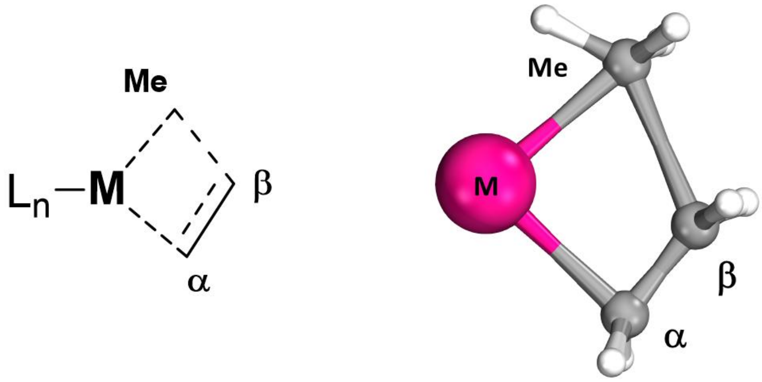

Figure S2. Chemdraw (left) and optimized structure (right) of the repeating unit of ACM and TSM model structures showing the coding employed. Optimized structure referring to the TSM of the Zr-based metallocene.

The python scripts used for file conversion and descriptors collection are available in the "Python_scripts.zip" folder. A brief explanation of how each script can be used is provided at the end of this document (**Python Scripts** section).

2. Descriptor evaluation and collection

All the optimizations and wavefunction calculations were performed using Gaussain 16 Revision A.03.[5] A small-core effective core pseudopotential (MDF28) was used for Y, Zr and Hf.[6,7] Geometries were fully optimized at the TPSSh/cc-pVDZ-(PP) level of theory.[6–10] The nature of all stationary points was confirmed by vibrational analysis showing no imaginary frequency for chloride precursors, methyl precursors and ACM, and one imaginary frequency associated to the insertion reaction for TSM. Standard convergence criteria and grid sizes were employed for all the calculations, except for the methyl precursor of the Y-based phosphinimide, for which a Superfine grid was required to locate the minimum. The density fitting approximation (Resolution of Identity, RI) was used.[11–14] Transition states were located using a suitable guess and the Berny algorithm (Opt = TS), occasionally preceded by a relaxed potential energy scan to arrive at a suitable transition-state guess.[15] The geometries of all the optimized structures are available in the "Structures.xyz" file.

The electronic descriptors were evaluated on the optimized geometries according to the following protocols:

- **Mulliken,**[16] **Hirshfeld,**[17] **CM5,**[18] **and ESP** [19] **charges**: the wavefunction was calculated at the MN15-L/cc-pVTZ-(PP) level of theory,[20] and the descriptors were calculated using the Gaussian 16 built in functions.
- **NPA charges and NBO-Wiberg Bond Indexes**: the wavefunction was calculated at the MN15-L/cc-pVTZ-(PP) level of theory, and the descriptors were calculated using NBO 7.0 integrated in Gaussian 16.[21–23]
- **IBO and QTAIM charges, IBO-Wiberg Bond Indexes and Bond Compositions**: the wavefunction was calculated at the MN15-L/def2-TZVP level of theory, printing the molecular orbitals composition in the output file. The Gaussian output file was then converted in Molden format using the "Gaussian2Molden.py" script. The descriptors were calculated on IboView running the IAO/IBO analysis (Orbital localization: IBO exponent 2; Orbital Division: As input wf) and the Formal Charges analysis (Real Space via TFVC; Integration Grid: grid{accu_ 1e-5}).[24–26]

For each geometry the atom list was sorted so that the repeating unit of the model structure was displayed first, to facilitate descriptors collection. The various fragments were ordered as follows (**Figure S3**):

- MCl_x: 1 – Metal ; 2 – Chlorine; 3 – Chlorine
- MMe_x: 1 – Metal ; 2 – Carbon (Me1) ; 3/4/5 – Hydrogens (Me1) ; 6 – Carbon (Me2) ; 7/8/9 – Hydrogens (Me2)
- ACM/TSM: 1 – Metal ; 2 – Carbon (Me) ; 3/4/5 – Hydrogens (Me) ; 6 – Carbon (Eth, α) ; 7 – Carbon (Eth, β) ; 8/9/10/11 – Hydrogens (Eth)

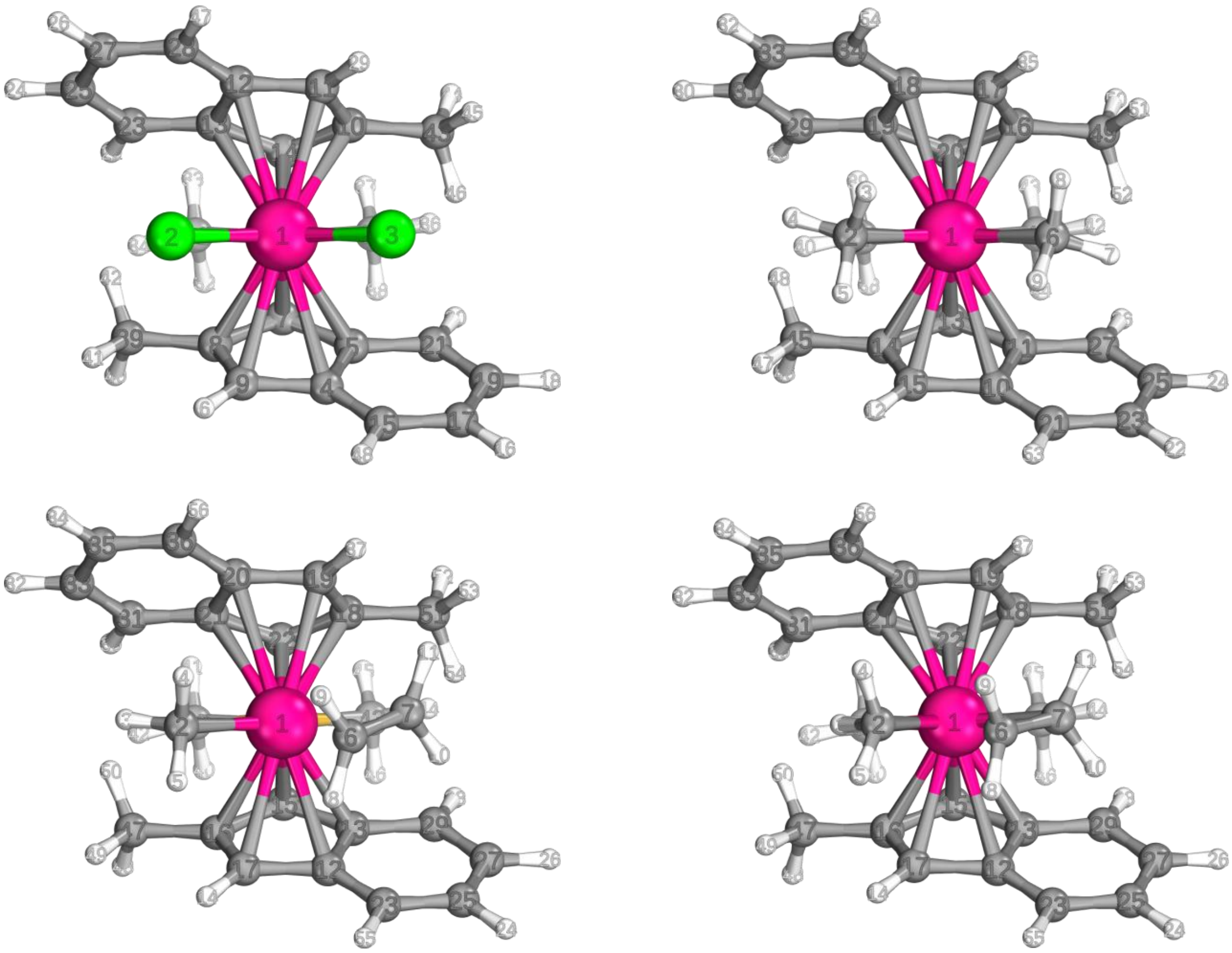

Figure S3. Optimized structures for the Zr-Metallocene dichloride precursor (top-left), dimethyl precursor (top-right), ACM (bottom-left) and TSM (bottom-right) showing the atom sorting adopted for the repeating units.

The descriptors were then collected directly from the Gaussian output files or from the IboView log files using the python scripts “Gaussian_Descriptors_MCl2.py”, “Gaussian_Descriptors_MMe2.py”, “Gaussian_Descriptors_Me_Eth.py”, “IBO_Descriptors_MCl2.py”, “IBO_Descriptors_MMe2.py” and “IBO_Descriptors_Me_Eth.py”.

3. Correlation between different model structures

The coefficients of determination (R^2) for the linear correlation of the electronic descriptors evaluated on different model structures are reported in **Tables S1-S3**.

Table S2. Coefficients of determination for the correlation of metal and ligand charges evaluated on different model structures.

		q_M				q_L			
	Model Structure	MCl_x	MMe_x	ACM	TSM	MCl_x	MMe_x	ACM	TSM
NPA	MCl_x	1.0000	0.6903	0.5033	0.5159	1.0000	0.9744	0.9493	0.9565
	MMe_x		1.0000	0.9104	0.9314		1.0000	0.9532	0.9455
	ACM			1.0000	0.9117			1.0000	0.9901
	TSM				1.0000				1.0000
Hirshfeld	MCl_x	1.0000	0.9884	0.4965	0.5324	1.0000	0.9707	0.8763	0.8699
	MMe_x		1.0000	0.5279	0.5782		1.0000	0.8533	0.8460
	ACM			1.0000	0.9801			1.0000	0.9993
	TSM				1.0000				1.0000
CM5	MCl_x	1.0000	0.9937	0.8369	0.8754	1.0000	0.3445	0.8716	0.8693
	MMe_x		1.0000	0.7780	0.8221		1.0000	0.6617	0.6564
	ACM			1.0000	0.9948			1.0000	0.9992
	TSM				1.0000				1.0000
Mulliken	MCl_x	1.0000	0.8851	0.9221	0.9087	1.0000	0.8873	0.7947	0.7925
	MMe_x		1.0000	0.8778	0.8249		1.0000	0.5764	0.5728
	ACM			1.0000	0.9825			1.0000	0.9993
	TSM				1.0000				1.0000
ESP	MCl_x	1.0000	0.6361	0.7681	0.7246	1.0000	0.8562	0.9192	0.9215
	MMe_x		1.0000	0.7591	0.7344		1.0000	0.7708	0.8244
	ACM			1.0000	0.9384			1.0000	0.9689
	TSM				1.0000				1.0000
IBO	MCl_x	1.0000	0.9995	0.9979	0.9985	1.0000	0.9929	0.9571	0.9608
	MMe_x		1.0000	0.9985	0.9991		1.0000	0.9220	0.9264
	ACM			1.0000	0.9995			1.0000	0.9984
	TSM				1.0000				1.0000
QTAIM	MCl_x	1.0000	0.9935	0.9982	0.9979	1.0000	0.9592	0.7502	0.7342
	MMe_x		1.0000	0.9903	0.9926		1.0000	0.8703	0.8631
	ACM			1.0000	0.9992			1.0000	0.9950
	TSM				1.0000				1.0000

Table S3. Coefficients of determination for the correlation of Wiberg Bond Indexes evaluated on different model structures.

	Wiberg Bond Index (NBO)				Wiberg Bond Index (IBO)			
Model Structure	**MCl_x**	**MMe_x**	**ACM**	**TSM**	**MCl_x**	**MMe_x**	**ACM**	**TSM**
MCl_x	1.0000	0.8452	0.7811	0.7369	1.0000	0.9715	0.9531	0.9113
MMe_x		1.0000	0.9485	0.9108		1.0000	0.9881	0.9501
ACM			1.0000	0.9123			1.0000	0.9475
TSM				1.0000				1.0000

M-Cl Wiberg Bond Indexes were considered for chloride precursors, while M-Me bonds were considered for methyl precursors, ACM and TSM. For Group 4 precursors averages values of the two chlorides/methyls were used.

Table S4. Coefficients of determination for the correlation of IBO Bond Compositions evaluated on different model structures.

	Wiberg Bond Index (NBO)			
Model Structure	**MCl_x**	**MMe_x**	**ACM**	**TSM**
MCl_x	1.0000	0.9987	0.9827	0.9079
MMe_x		1.0000	0.9812	0.9120
ACM			1.0000	0.8758
TSM				1.0000

M-Cl Wiberg Bond Compositons were considered for chloride precursors, while M-Me bonds were considered for methyl precursors, ACM and TSM. The values refer to the contribution of the chloride or methyl carbon to the bond. For Group 4 precursors averages values of the two chlorides/methyls were used.

4. Descriptors clustering analysis

The clustering analysis of partial charges for TSM and of Wiberg Bond Indexes for ACM was carried out plotting each datapoint in a scatterplot with a colour and shape indicating the corresponding metal and ligand and checking visually the distribution of ligand and metal datapoints. In the case of methyl, ethene, α carbon and β carbon, hydrogen charges were summed into those of the corresponding heavy atom. The IBO Wiberg Bond Index for the methyl carbon – β carbon bond could not be analyzed being under the printing threshold for most of the structures. The clustering and spacing analysis for the complete descriptors set is summarized in **Table S4** and **Table S5**. The plots used for the analysis are reported in **Figure S4-S28**.

Table S5. Summary of clustering analysis for Wiberg Bond Indexes and Bond composition evaluated on ACM.

Method	Descriptor	Total Spacing	Max Ligand Spacing	Max Metal Spacing	Groups Overlap	Series Overlap	Dominant Influence	Clustering
Wiberg Bond Indices (calculated on ACM)								
IBO	$WBI_{M\text{-}Me}$	0.604	0.117	0.604	Yes	No	Metal	**1**: Sc; **2**: Ti; **3**: Y, Zr, Hf
	$WBI_{M\text{-}\alpha}$	0.201	0.101	0.201	Yes	Yes	Metal	**1**: Ti; **2**: Sc, Y, Zr, Hf
	$WBI_{\alpha\text{-}\beta}$	0.239	0.111	0.239	Yes	Yes	Even	Absent
	$BC_{M\text{-}Me}$	0.525	0.079	0.525	No	No	Metal	**1**: Sc; **2**: Ti; **3**: Y, Zr, Hf
NBO	$WBI_{M\text{-}Me}$	0.390	0.091	0.390	No	Yes	Metal	Absent
	$WBI_{M\text{-}\alpha}$	0.202	0.099	0.202	No	Yes	Metal	Absent
	$WBI_{\alpha\text{-}\beta}$	0.228	0.105	0.228	No	Yes	Metal	Absent
	$WBI_{M\text{-}\beta}$	0.143	0.141	0.142	Yes	Yes	Metal	Absent

Table S6. Summary of clustering analysis for partial charges evaluated on TSM.

Method	Descriptor	Total Spacing	Max Ligand Spacing	Max Metal Spacing	Groups Overlap	Series Overlap	Dominant Influence	Clustering
IBO	q_M	2.122	0.158	2.122	Yes	No	Metal	**1**: Sc, Ti; **2**: Y; **3**: Zr, Hf
	q_L	1.426	0.215	1.426	Yes	No	Metal	**1**: Sc; **2**: Ti; **3**: Y, Zr, Hf
	q_{Me}	0.352	0.058	0.352	Yes	No	Metal	**1**: Sc, Ti; **2**: Y, Zr, Hf
	q_{Ethene}	0.423	0.062	0.423	Yes	No	Metal	**1**: Sc; **2**: Ti; **3**: Y, Zr, Hf
	q_α	0.355	0.057	0.354	Yes	No	Metal	**1**: Sc; **2**: Ti; **3**: Y, Zr, Hf
	q_β	0.087	0.017	0.076	Yes	Yes	Even	Absent
QTAIM	q_M	0.821	0.288	0.685	Yes	Yes	Even	Absent
	q_L	1.070	0.308	0.907	Yes	Yes	Even	Absent
	q_{Me}	0.160	0.056	0.160	Yes	Yes	Metal	Absent
	q_{Ethene}	0.282	0.061	0.282	Yes	Yes	Metal	**1**: Ti; **2**: Sc, Y, Zr, Hf
	q_α	0.191	0.035	0.179	Yes	Yes	Metal	**1**: Ti; **2**: Sc, Y, Zr, Hf
	q_β	0.129	0.045	0.103	Yes	Yes	Even	Absent
NPA	q_M	0.859	0.395	0.512	Yes	Yes	Even	Absent
	q_L	1.046	0.387	0.914	Yes	Yes	Even	Absent
	q_{Me}	0.192	0.109	0.166	Yes	Yes	Even	Absent
	q_{Ethene}	0.262	0.038	0.246	No	Yes	Metal	**1**: Sc, Y; **2**: Ti, Zr, Hf
	q_α	0.197	0.040	0.189	Yes	Yes	Metal	Absent
	q_β	0.095	0.021	0.081	No	Yes	Metal	**1**: Sc, Y; **2**: Ti, Zr, Hf
ESP	q_M	1.342	0.954	0.784	Yes	Yes	Even	Absent
	q_L	1.795	0.893	1.267	Yes	Yes	Even	Absent
	q_{Me}	0.263	0.071	0.234	No	Yes	Metal	**1**: Sc, Y; **2**: Ti, Zr, Hf
	q_{Ethene}	0.326	0.026	0.325	No	Yes	Metal	**1**: Sc, Y; **2**: Ti, Zr, Hf
	q_α	0.311	0.087	0.283	No	Yes	Even	**1**: Sc, Y; **2**: Ti, Zr, Hf
	q_β	0.178	0.079	0.119	Yes	Yes	Even	Absent
Mulliken	q_M	0.745	0.686	0.291	Yes	Yes	Even	Absent
	q_L	1.177	0.654	0.829	No	Yes	Even	Absent
	q_{Me}	0.260	0.092	0.224	No	Yes	Metal	Absent
	q_{Ethene}	0.290	0.109	0.223	No	Yes	Metal	Absent
	q_α	0.175	0.094	0.118	Yes	Yes	Even	Absent
	q_β	0.125	0.045	0.122	No	Yes	Metal	**1**: Sc, Y; **2**: Ti, Zr, Hf
Hirshfeld	q_M	0.242	0.145	0.151	Yes	Yes	Even	Absent
	q_L	0.979	0.248	0.850	No	Yes	Metal	**1**: Sc, Y; **2**: Ti, Zr, Hf
	q_{Me}	0.140	0.072	0.140	No	Yes	Metal	**1**: Sc, Y; **2**: Ti, Zr, Hf
	q_{Ethene}	0.242	0.055	0.190	No	Yes	Metal	**1**: Sc, Y; **2**: Ti, Zr, Hf
	q_α	0.149	0.041	0.125	No	Yes	Metal	Absent
	q_β	0.101	0.027	0.086	No	Yes	Metal	**1**: Sc, Y; **2**: Ti, Zr, Hf
CM5	q_M	0.532	0.345	0.248	Yes	Yes	Even	Absent
	q_L	1.164	0.463	0.871	No	Yes	Even	Absent
	q_{Me}	0.141	0.072	0.141	No	Yes	Even	**1**: Sc, Y; **2**: Ti, Zr, Hf
	q_{Ethene}	0.270	0.064	0.223	No	Yes	Metal	**1**: Sc, Y; **2**: Ti, Zr, Hf
	q_α	0.169	0.048	0.150	No	Yes	Metal	Absent
	q_β	0.101	0.027	0.085	No	Yes	Metal	**1**: Sc, Y; **2**: Ti, Zr, Hf

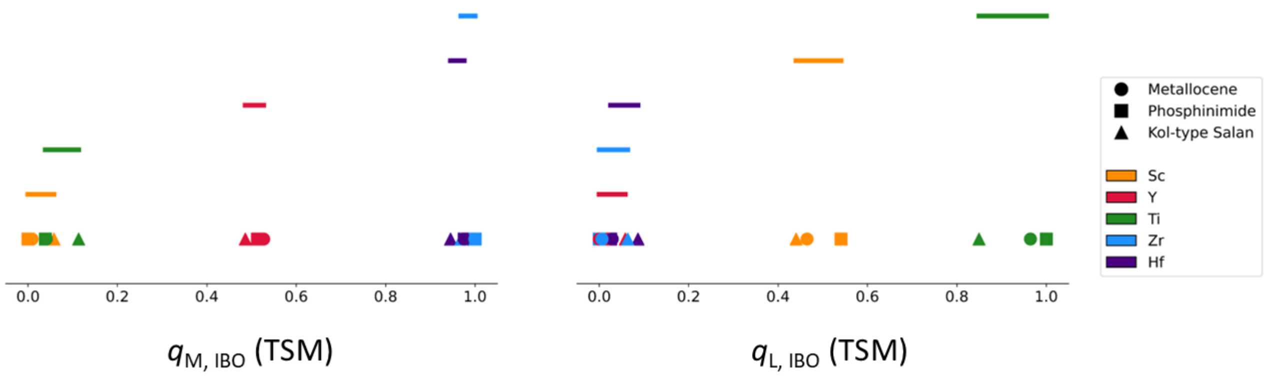

Figure S4. Spacing plots of metal (left) and ligand (right) IBO charges calculated on TSM. Highlighted regions indicate the descriptor space covered by each metal. Descriptors values were normalized between 0 and 1.

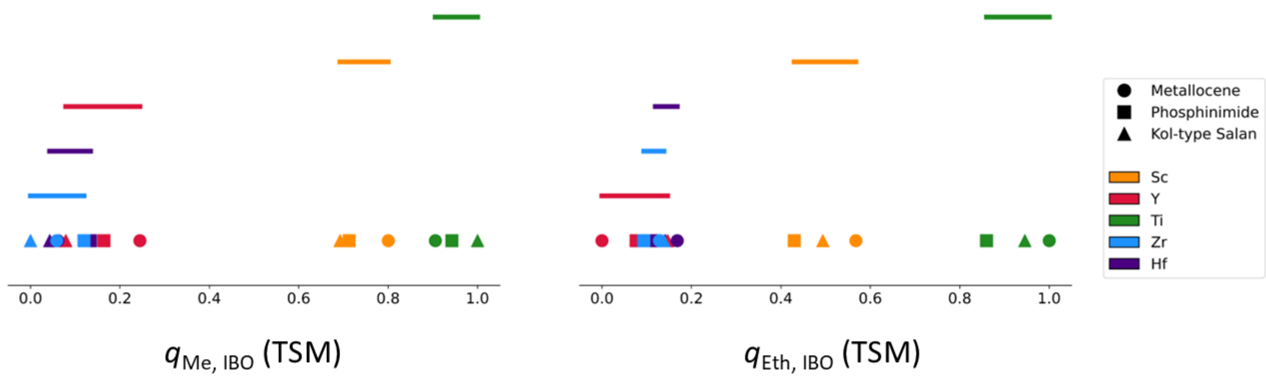

Figure S5. Spacing plots of methyl (left) and ethene (right) IBO charges calculated on TSM. Highlighted regions indicate the descriptor space covered by each metal. Descriptors values were normalized between 0 and 1.

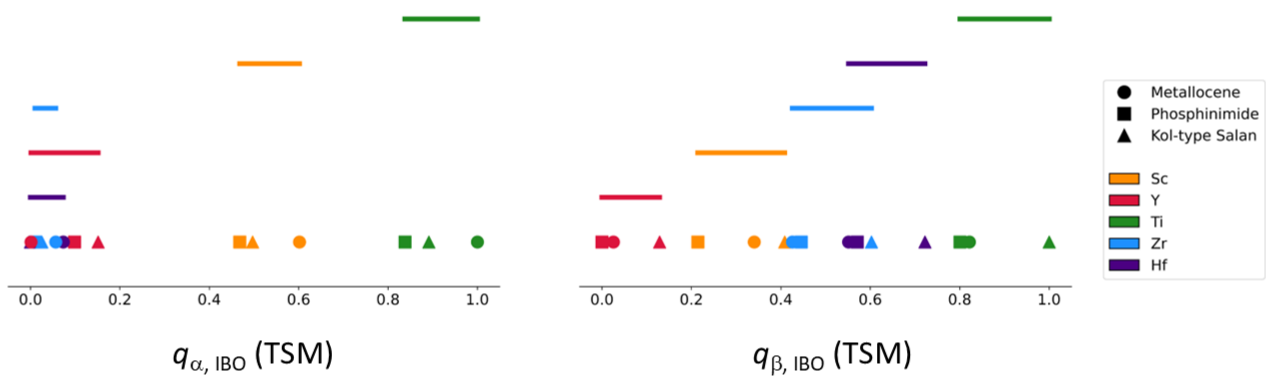

Figure S6. Spacing plots of α (left) and β (right) methylenes IBO charges calculated on TSM. Highlighted regions indicate the descriptor space covered by each metal. Descriptors values were normalized between 0 and 1.

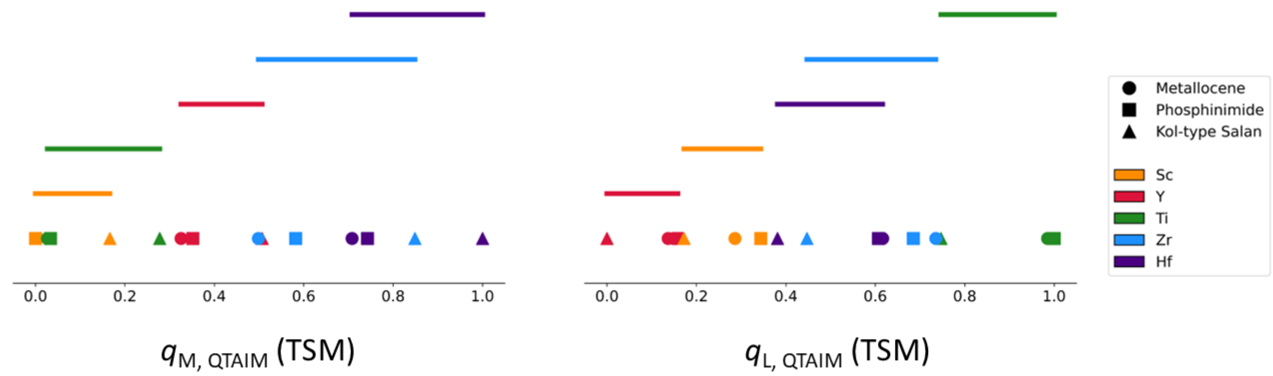

Figure S7. Spacing plots of metal (left) and ligand (right) QTAIM charges calculated on TSM. Highlighted regions indicate the descriptor space covered by each metal. Descriptors values were normalized between 0 and 1.

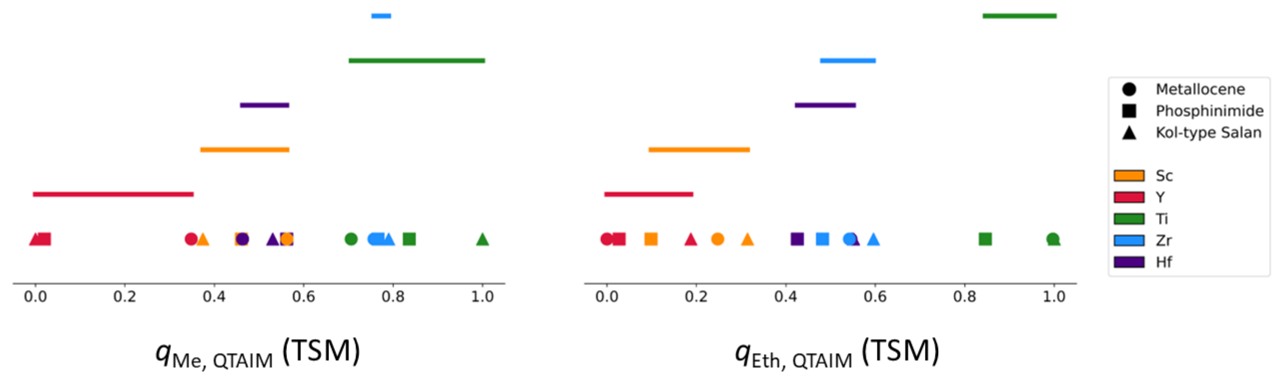

Figure S8. Spacing plots of methyl (left) and ethene (right) QTAIM charges calculated on TSM. Highlighted regions indicate the descriptor space covered by each metal. Descriptors values were normalized between 0 and 1.

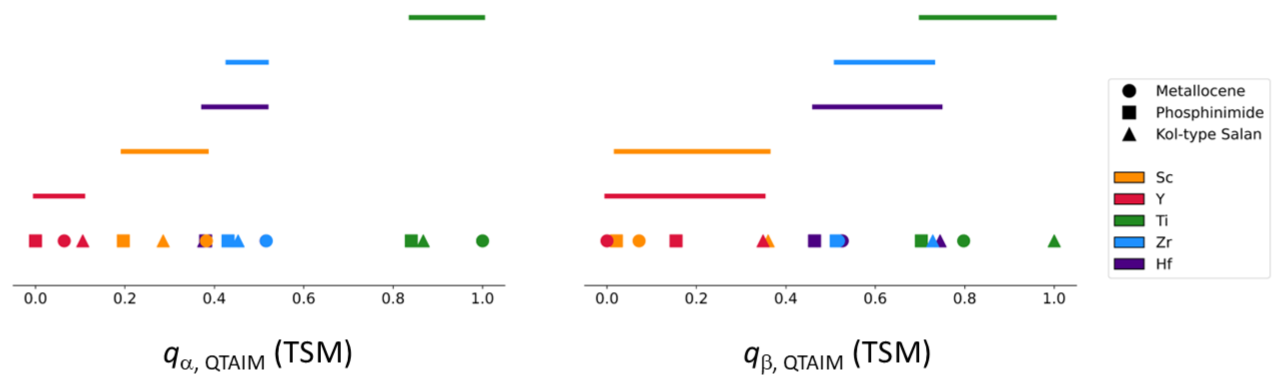

Figure S9. Spacing plots of α (left) and β (right) methylenes QTAIM charges calculated on TSM. Highlighted regions indicate the descriptor space covered by each metal. Descriptors values were normalized between 0 and 1.

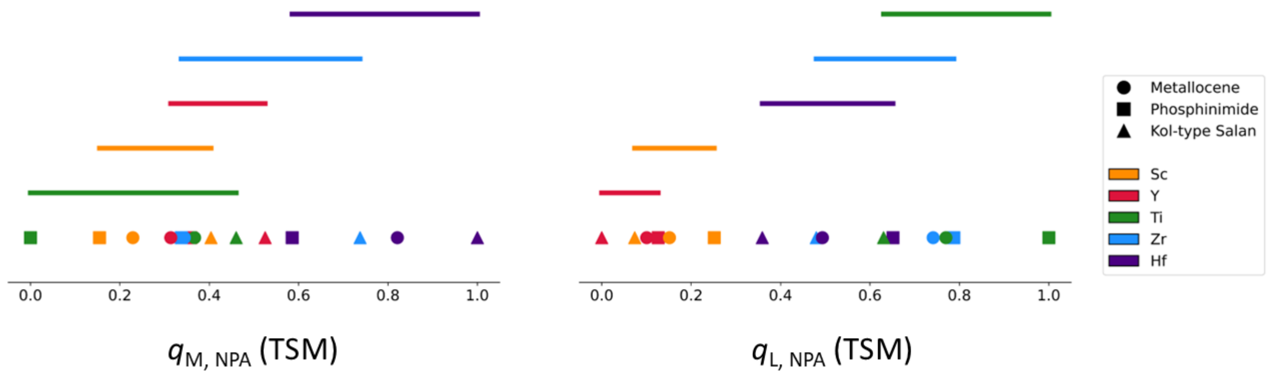

Figure S10. Spacing plots of metal (left) and ligand (right) NPA charges calculated on TSM. Highlighted regions indicate the descriptor space covered by each metal. Descriptors values were normalized between 0 and 1.

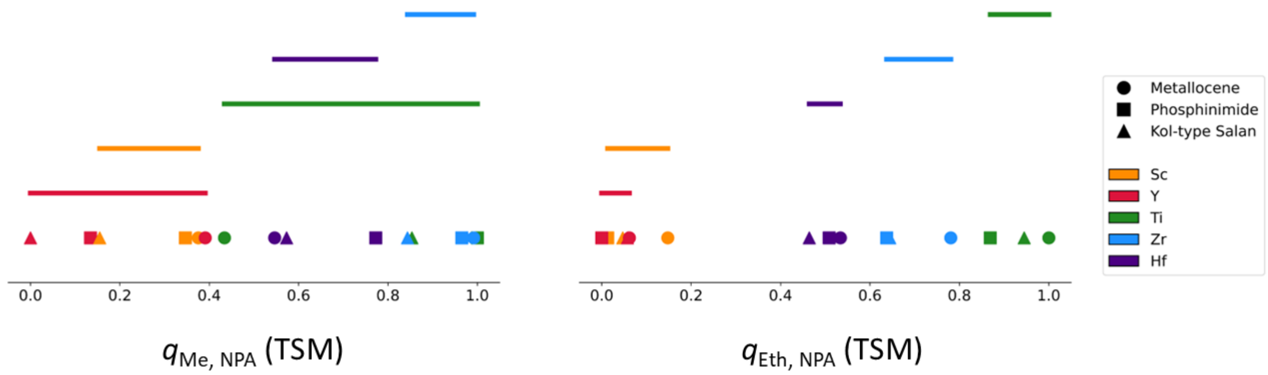

Figure S11. Spacing plots of methyl (left) and ethene (right) NPA charges calculated on TSM. Highlighted regions indicate the descriptor space covered by each metal. Descriptors values were normalized between 0 and 1.

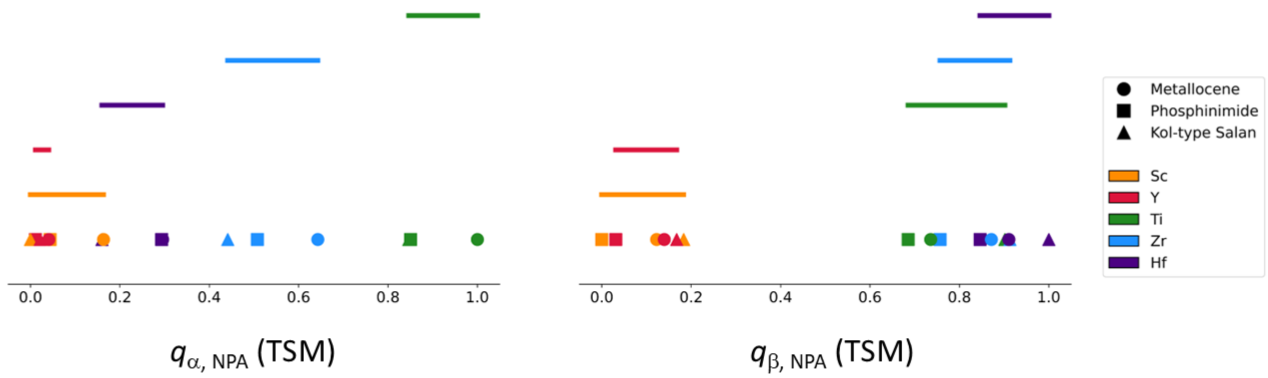

Figure S12. Spacing plots of α (left) and β (right) methylenes NPA charges calculated on TSM. Highlighted regions indicate the descriptor space covered by each metal. Descriptors values were normalized between 0 and 1.

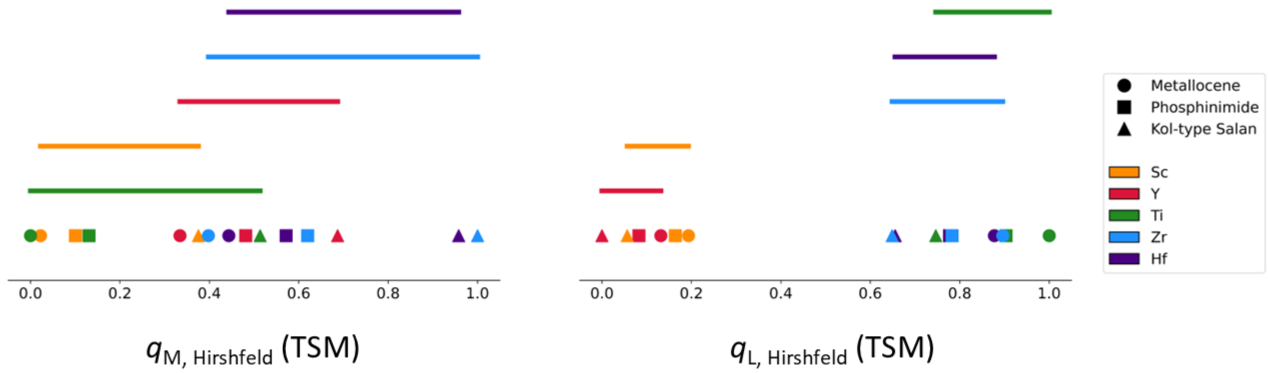

Figure S13. Spacing plots of metal (left) and ligand (right) Hirshfeld charges calculated on TSM. Highlighted regions indicate the descriptor space covered by each metal. Descriptors values were normalized between 0 and 1.

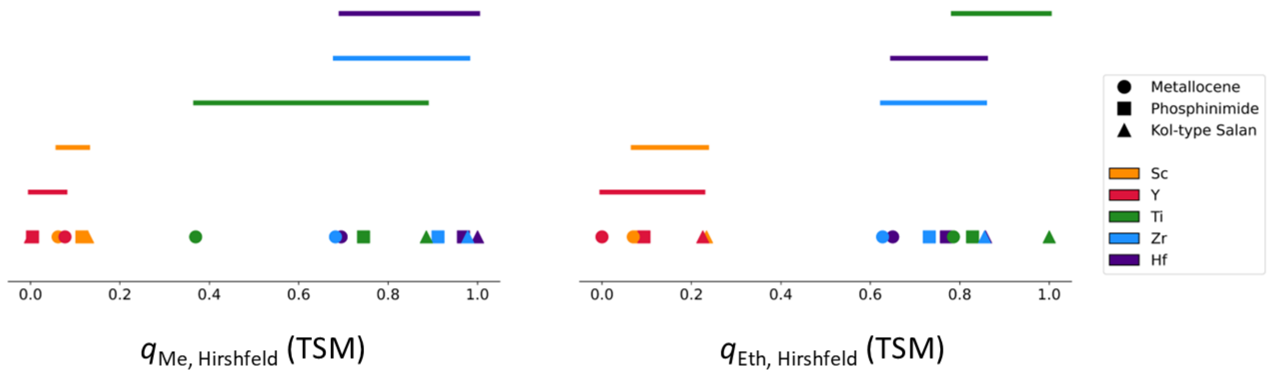

Figure S14. Spacing plots of methyl (left) and ethene (right) Hirshfeld charges calculated on TSM. Highlighted regions indicate the descriptor space covered by each metal. Descriptors values were normalized between 0 and 1.

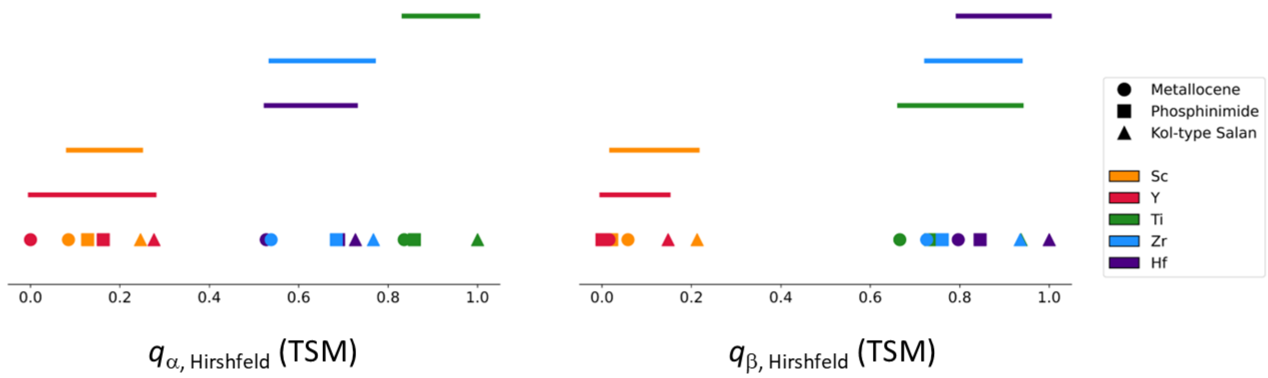

Figure S15. Spacing plots of α (left) and β (right) methylenes Hirshfeld charges calculated on TSM. Highlighted regions indicate the descriptor space covered by each metal. Descriptors values were normalized between 0 and 1.

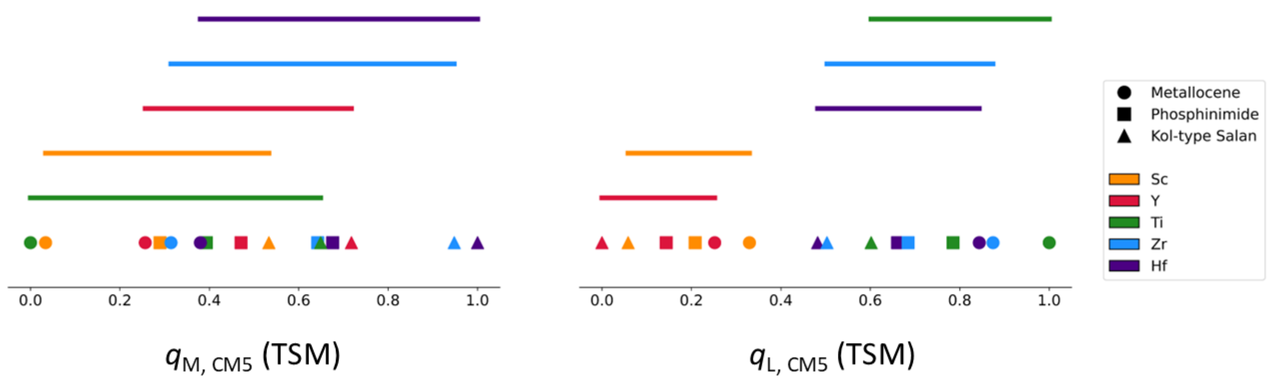

Figure S16. Spacing plots of metal (left) and ligand (right) CM5 charges calculated on TSM. Highlighted regions indicate the descriptor space covered by each metal. Descriptors values were normalized between 0 and 1.

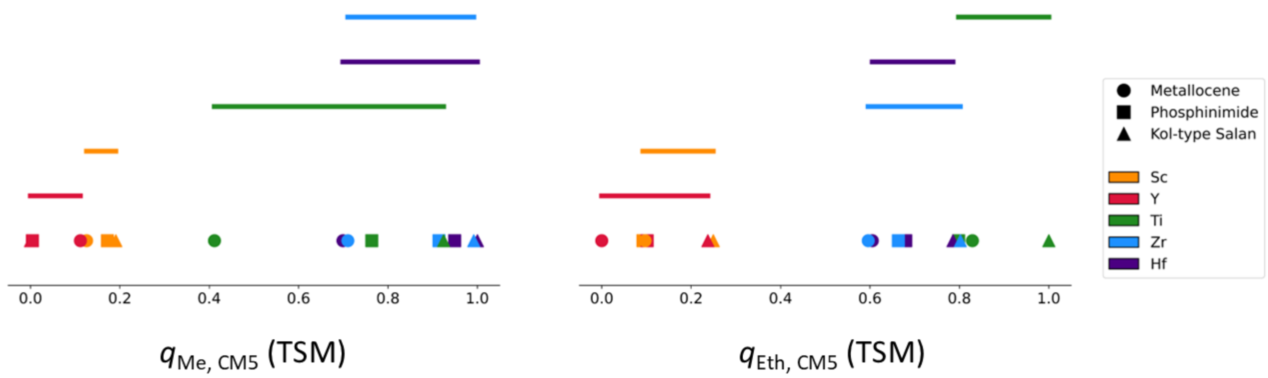

Figure S17. Spacing plots of methyl (left) and ethene (right) CM5 charges calculated on TSM. Highlighted regions indicate the descriptor space covered by each metal. Descriptors values were normalized between 0 and 1.

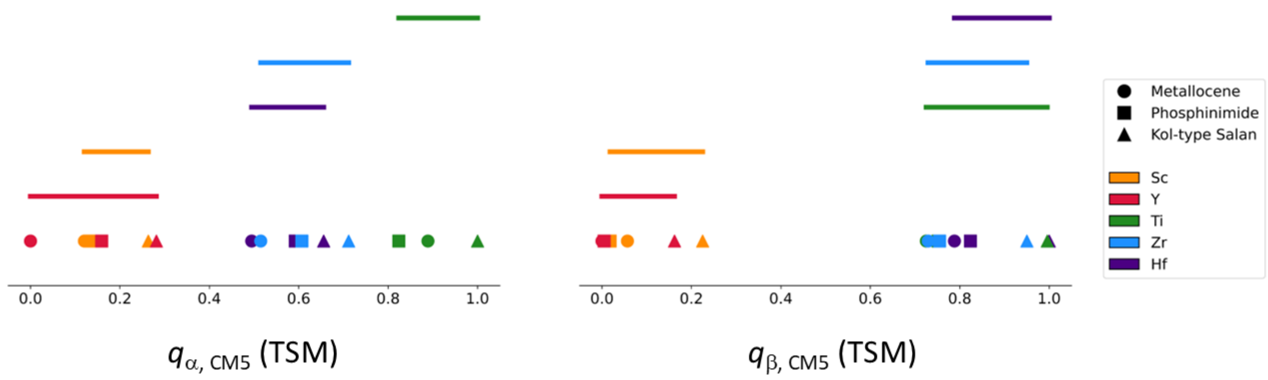

Figure S18. Spacing plots of α (left) and β (right) methylenes CM5 charges calculated on TSM. Highlighted regions indicate the descriptor space covered by each metal. Descriptors values were normalized between 0 and 1.

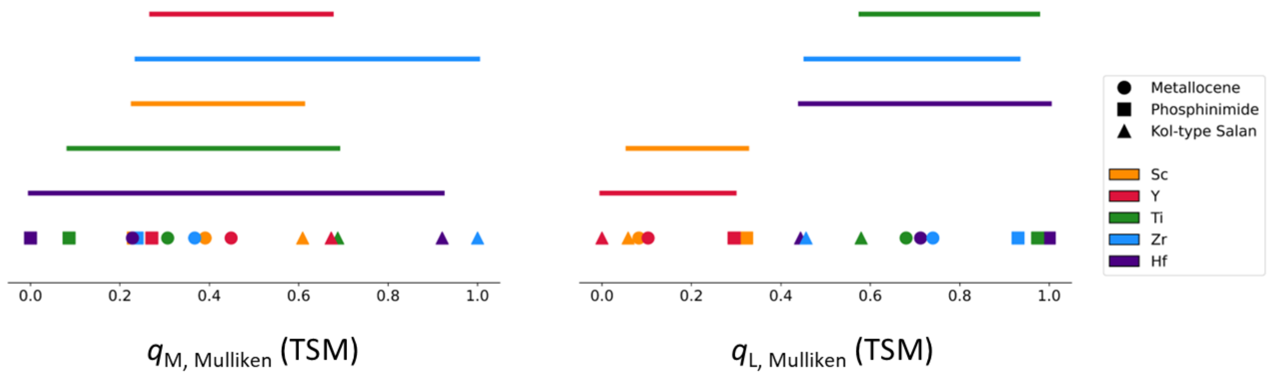

Figure S19. Spacing plots of metal (left) and ligand (right) Mulliken charges calculated on TSM. Highlighted regions indicate the descriptor space covered by each metal. Descriptors values were normalized between 0 and 1.

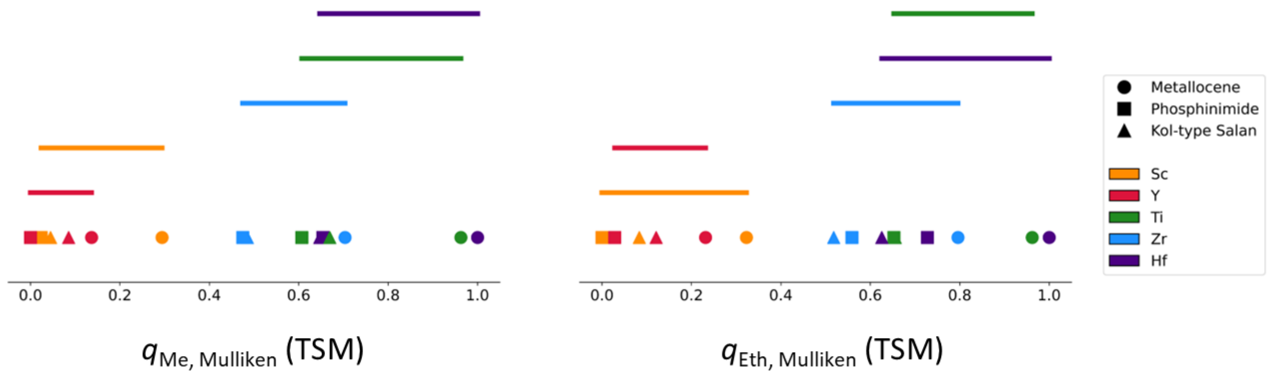

Figure S20. Spacing plots of methyl (left) and ethene (right) Mulliken charges calculated on TSM. Highlighted regions indicate the descriptor space covered by each metal. Descriptors values were normalized between 0 and 1.

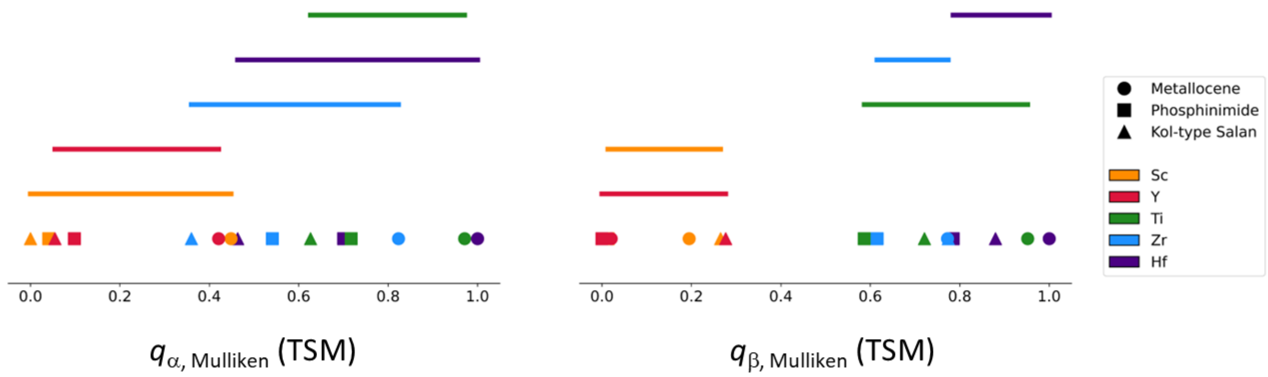

Figure S21. Spacing plots of α (left) and β (right) methylenes Mulliken charges calculated on TSM. Highlighted regions indicate the descriptor space covered by each metal. Descriptors values were normalized between 0 and 1.

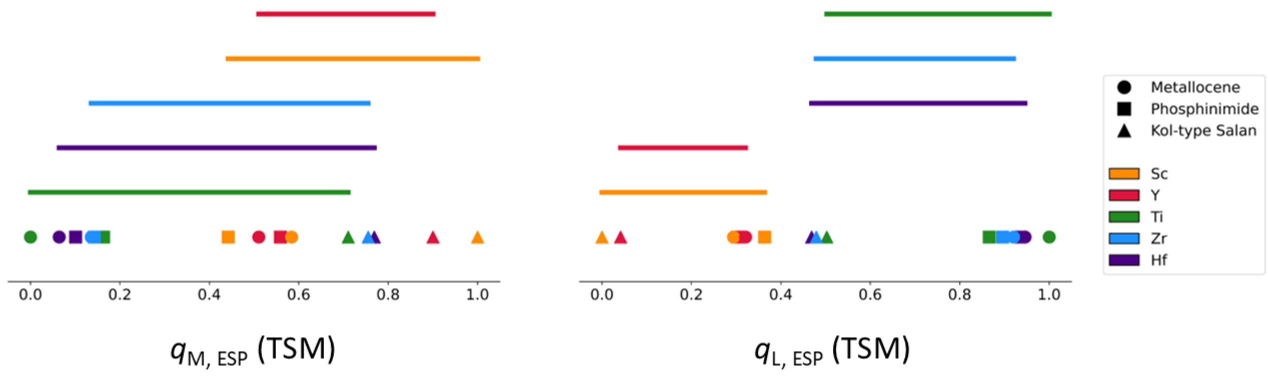

Figure S22. Spacing plots of metal (left) and ligand (right) ESP charges calculated on TSM. Highlighted regions indicate the descriptor space covered by each metal. Descriptors values were normalized between 0 and 1.

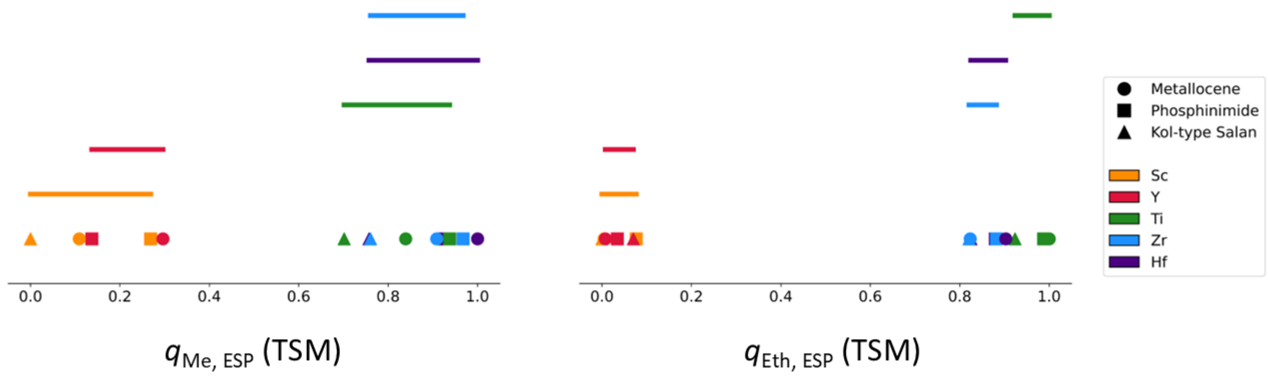

Figure S23. Spacing plots of methyl (left) and ethene (right) ESP charges calculated on TSM. Highlighted regions indicate the descriptor space covered by each metal. Descriptors values were normalized between 0 and 1.

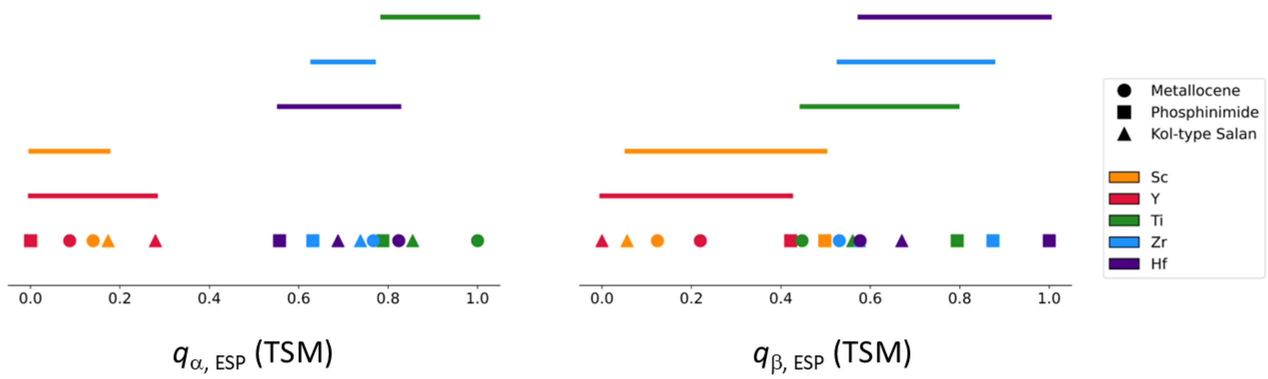

Figure S24. Spacing plots of α (left) and β (right) methylenes ESP charges calculated on TSM. Highlighted regions indicate the descriptor space covered by each metal. Descriptors values were normalized between 0 and 1.

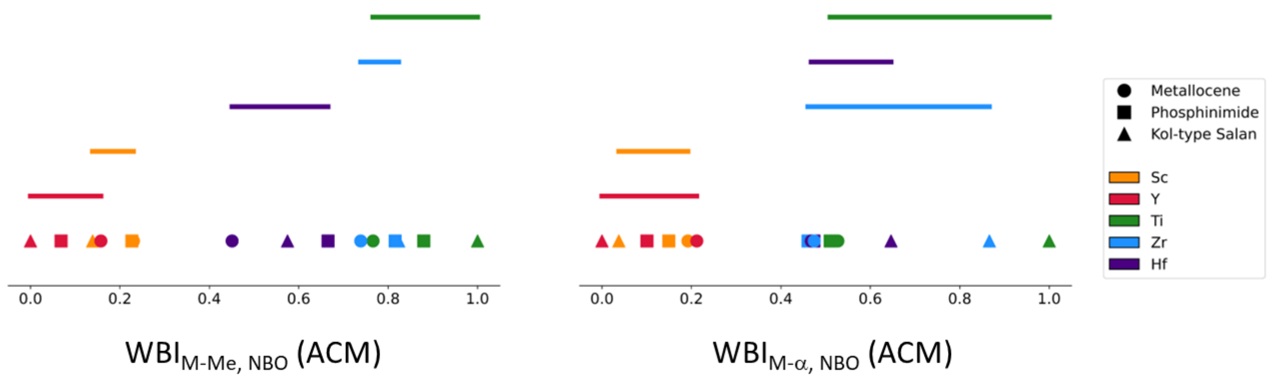

Figure S25. NBO Wiberg Bond Indexes for M – Me (left) and M – α (right) bonds calculated on ACM. Highlighted regions indicate the descriptor space covered by each metal. Descriptors values were normalized between 0 and 1.

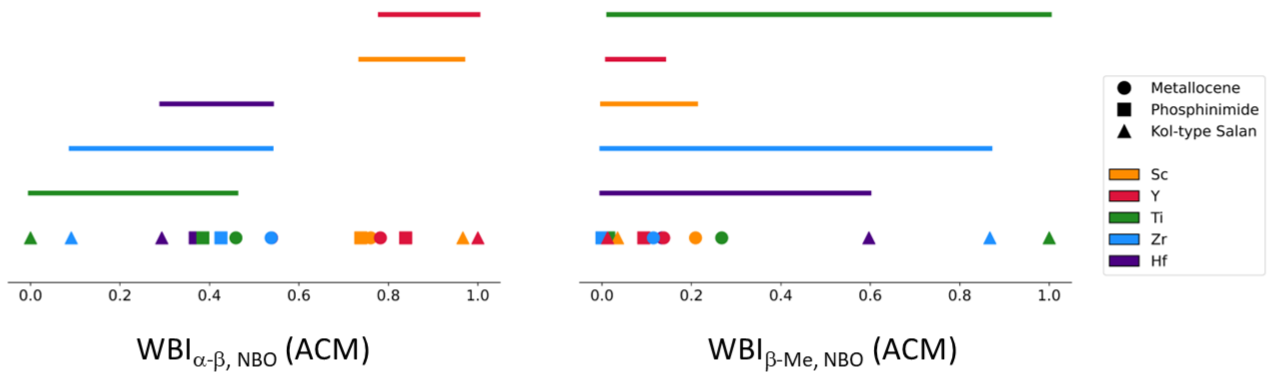

Figure S26. NBO Wiberg Bond Indexes for α– β (left) and Me – β (right) bonds calculated on ACM. Highlighted regions indicate the descriptor space covered by each metal. Descriptors values were normalized between 0 and 1.

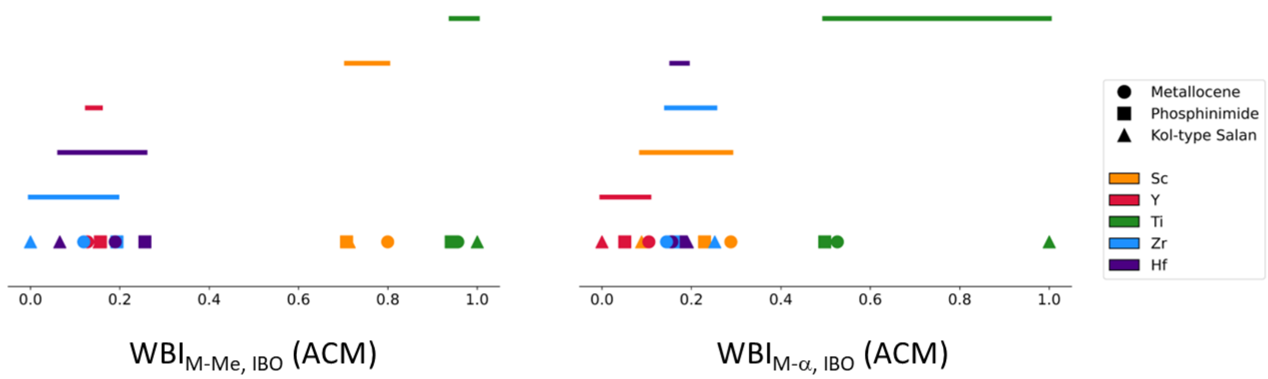

Figure S27. IBO Wiberg Bond Indexes for M – Me (left) and M – α (right) bonds calculated on ACM. Highlighted regions indicate the descriptor space covered by each metal. Descriptors values were normalized between 0 and 1.

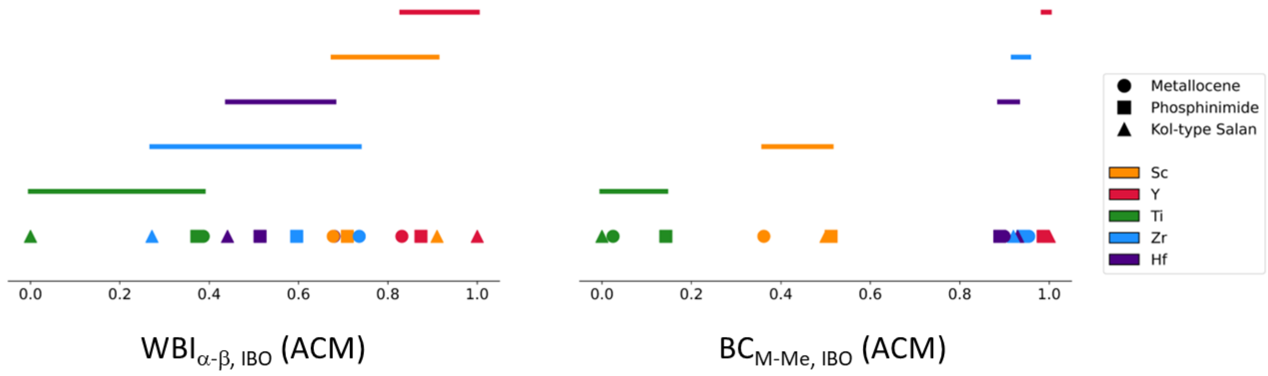

Figure S28. IBO Wiberg Bond Indexes for α carbon – β carbon bond (left) and methyl contribution to the IBO Bond Composition for the M-Me bond calculated on ACM. Highlighted regions indicate the descriptor space covered by each metal. Descriptors values were normalized between 0 and 1.

5. Python scripts use

The "Python_scripts.zip" folder contains python scripts which allow automatic file conversion and descriptors collection. A brief explanation of how to use each script is reported below.

Gaussian2Molden.py: converts all the .out files in the current working directory into .molden files, emulating the process of opening the .out files on Molden and writing a .molden file. The script has been written specifically for energy caluclations (not optimizations) obtained using these additional keywords:

#p IOP(6/7=3)

The .molden files contain all the information about molecular geometry, basis set and molecular orbital coefficients, but lack the details on the SCF cycles and energies (which is instead present when converting the file using Molden). The .molden files require dos2unix transformation in order to be readable by iBOview. The .molden files are located into an expressly created directory named "Molden_files". The script will fail if a directory named "Molden_files" is already existing in the current working directory.

Gaussian_decsriptors_MCl2.py: collects a series of electronic descriptors from all the .out files in the current working directory. The script has been written specifically for chloride precursors and in order to work correctly in the .out files the atoms must be ordered as shown in **Figure S3, top-left**. The collected descriptors are: Mulliken charges, Hirshfeld charges, CM5 charges, ESP charges, NPA charges and Wiberg bond indexes. The charges are collected for the MCl_x fragment and the Wiberg bond indexes for the M-Cl bond(s). Before starting the collection, the script will ask which of the available descriptors are required. The descriptors are then saved in individual CSV files located into an expressly created directory named "OUTPUT". The script will fail if a directory named "OUTPUT" is already existing in the current working directory.

Gaussian_decsriptors_MMe2.py: collects a series of electronic descriptors from all the .out files in the current working directory. The script has been written specifically for methyl precursors and in order to work correctly in the original .out files the atoms must be ordered as shown in **Figure S3, top-right**. The descriptors collected are: Mulliken charges, Hirshfeld charges, CM5 charges, ESP charges, NPA charges and Wiberg bond indexes. The charges are collected for the MMe_x fragment and the Wiberg bond indexes for the M-C bond(s). Before starting the collection, the script will ask which of the available descriptors are required. The descriptors are then saved in individual CSV files located into an expressly created directory named "OUTPUT". The script will fail if a directory named "OUTPUT" is already existing in the current working directory.

Gaussian_decsriptors_Me_Eth.py: collects a series of electronic descriptors from all the .out files in the current working directory. The script has been written specifically for the TS or pre-insertion complexes for the insertion of ethene into a M-Me bond. In order to work correctly in the original .out files the atoms must be ordered as shown in **Figure S3, bottom-left** and **bottom-right**. The descriptors collected are: Mulliken charges, Hirshfeld charges, CM5 charges, ESP charges, NPA charges and Wiberg bond indexes. The charges are collected for the M-Me-Ethene fragment and the Wiberg bond indexes for the M-Me, M-α, β-Me, α=β bonds. Before starting the collection, the script will ask which of the available descriptors are required. The descriptors are then saved in individual CSV files located into an expressly created directory named "OUTPUT". The script will fail if a directory named "OUTPUT" is already existing in the current working directory.

IBO_decsriptors_MCl2.py: collects a series of electronic descriptors from all the .scf-log.txt (for standard IBO analysis) and .eos-log.txt (for QTAIM analysis) files in the current working directory. The script has been written specifically for chloride precursors and in order to work correctly in the original .scf-log.txt and .eos-log.txt files the atoms must be ordered as shown in **Figure S3, top-left**. The descriptors collected are: IBO charges, Wiberg bond indexes, Bond Orbital Composition and QTAIM charges. The charges are collected for the MCl_x fragment, the Wiberg bond indexes for the M-Cl bond(s), while the Bond Orbital Composition is the chloride contribution to the M-Cl bond composition. Before starting the collection, the script will ask which of the available descriptors are required. The descriptors are then saved in individual CSV files located into an expressly created directory named "OUTPUT". The script will fail if a directory named "OUTPUT" is already existing in the current working directory.

IBO_decsriptors_MMe2.py: collects a series of electronic descriptors from all the .scf-log.txt (for standard IBO analysis) and .eos-log.txt (for QTAIM analysis) files in the current working directory. The script has been written specifically for methyl precursors and in order to work correctly in the original .scf-log.txt and .eos-log.txt files the atoms must be ordered as shown in **Figure S3, top-right**. The descriptors collected are: IBO charges, Wiberg bond indexes, Bond Orbital Composition and QTAIM charges. The charges are collected for the MMe_x fragment, Wiberg bond indexes for the M-C bond(s), while the Orbital Bond Composition is the carbon contribution to the M-Me bond. Before starting the collection, the script will ask which of the available descriptors are required. The descriptors are then saved in individual CSV files located into an expressly created directory named "OUTPUT". The script will fail if a directory named "OUTPUT" is already existing in the current working directory.

IBO_decsriptors_Me_Eth.py: collects a series of electronic descriptors from all the .scf-log.txt (for standard IBO analysis) and .eos-log.txt (for QTAIM analysis) files in the current working directory. The script has been written specifically for the TS or pre-insertion complexes for the insertion of ethene into a M-Me bond. In order to work correctly in the atoms must be ordered as shown in **Figure S3, bottom-left** and **bottom-right**. The descriptors collected are: IBO charges, Wiberg bond indexes, Bond Orbital Composition and QTAIM charges. The charges are collected for the M-Me-Ethene fragment and the Wiberg bond indexes for the M-

Me, M-α, β-Me, α=β bonds, while the Orbital Bond Composition is the carbon contribution to the M-Me bond. Before starting the collection, the script will ask which of the available descriptors are required. The descriptors are then saved in individual CSV files located into an expressly created directory named "OUTPUT". The script will fail if a directory named "OUTPUT" is already existing in the current working directory.

6. References

The references below as indexed in the Supporting Information are also cited in the manuscript. Please note that the order differs in the main manuscript.

1 A. Vittoria, G. P. Goryunov, V. V Izmer, D. S. Kononovich, O. V Samsonov, F. Zaccaria, G. Urciuoli, P. H. M. Budzelaar, V. Busico, A. Z. Voskoboynikov, D. V Uborsky, C. Ehm and R. Cipullo, *Polymers*, 2021, **13**, 2621.

2 D. V. Uborsky, M. I. Sharikov, G. P. Goryunov, K. M. Li, A. Dall'Anese, C. Zuccaccia, A. Vittoria, T. Iovine, G. Galasso, C. Ehm, A. Macchioni, V. Busico, A. Z. Voskoboynikov and R. Cipullo, *Inorg. Chem. Front.*, 2023, **10**, 6401–6406.

3 A. Vittoria, P. S. Kulyabin, G. Antinucci, A. N. Iashin, D. V. Uborsky, E. N. T. Cuthbert, P. H. M. Budzelaar, A. Z. Voskoboynikov, R. Cipullo, C. Ehm and V. Busico, *ACS Catal.*, 2023, **13**, 13151–13155.

4 L. Resconi, L. Cavallo, A. Fait and F. Piemontesi, *Chem. Rev.*, 2000, **100**, 1253–1346.

5 M. J. Frisch, G. W. Trucks, H. B. Schlegel, G. E. Scuseria, M. A. Robb, J. R. Cheeseman, G. Scalmani, V. Barone, G. A. Petersson, H. Nakatsuji, X. Li, M. Caricato, A. V Marenich, J. Bloino, B. G. Janesko, R. Gomperts, B. Mennucci, H. P. Hratchian, J. V Ortiz, A. F. Izmaylov, J. L. Sonnenberg, D. Williams-Young, F. Ding, F. Lipparini, F. Egidi, J. Goings, B. Peng, A. Petrone, T. Henderson, D. Ranasinghe, V. G. Zakrzewski, J. Gao, N. Rega, G. Zheng, W. Liang, M. Hada, M. Ehara, K. Toyota, R. Fukuda, J. Hasegawa, M. Ishida, T. Nakajima, Y. Honda, O. Kitao, H. Nakai, T. Vreven, K. Throssell, Jr. J. A. Montgomery, J. E. Peralta, F. Ogliaro, M. J. Bearpark, J. J. Heyd, E. N. Brothers, K. N. Kudin, V. N. Staroverov, T. A. Keith, R. Kobayashi, J. Normand, K. Raghavachari, A. P. Rendell, J. C. Burant, S. S. Iyengar, J. Tomasi, M. Cossi, J. M. Millam, M. Klene, C. Adamo, R. Cammi, J. W. Ochterski, R. L. Martin, K. Morokuma, O. Farkas, J. B. Foresman and D. J. Fox, Gaussian, Inc., Wallington CT, 2016.

6 P. Schwerdtfeger, *Chem. Phys. Chem.*, 2011, **12**, 3143–3155.

7 K. A. Peterson, D. Figgen, M. Dolg and H. Stoll, *J. Chem. Phys.*, 2007, **126**, 124101.

8 D. Figgen, K. A. Peterson, M. Dolg and H. Stoll, *J. Chem. Phys.*, 2009, **130**, 164108.

9 B. P. Pritchard, D. Altarawy, B. Didier, T. D. Gibson and T. L. Windus, *J. Chem. Inf. Model.*, 2019, **59**, 4814-4820.

10 N. B. Balabanov and K. A. Peterson, *J. Chem. Phys.*, 2005, **123**, 064107.

11 M. Feyereisen, G. Fitzgerald and A. Komornicki, *Chem. Phys. Lett.*, 1993, **208**, 359–363.

12 O. Vahtras, J. Almlöf and M. W. Feyereisen, *Chem. Phys. Lett.*, 1993, **213**, 514–518.

13 E. J. Baerends, D. E. Ellis and P. Ros, *Chem. Phys.*, 1973, **2**, 41–51.

14 J. L. Whitten, *J. Chem. Phys.*, 1973, **58**, 4496–4501.

15 The Berny algorithm was never fully published; see the Gaussian documentation for details.

16 R. S. Mulliken, *J. Chem. Phys.*, 1955, **23**, 1833–1840.

17 F. L. Hirshfeld, *Theoret. Chim. Acta*, 1977, **44**, 129–138.

18 A. V. Marenich, S. V. Jerome, C. J. Cramer and D. G. Truhlar, *J. Chem. Theory Comput.*, 2012, **8**, 527–541.

19 F. A. Momany, *J. Phys. Chem.*, 1978, **82**, 592–601.

20 H. S. Yu, X. He and D. G. Truhlar, *J. Chem. Theory Comput.*, 2016, **12**, 1280–1293.

21 J. P. Foster and F. Weinhold, *J. Am. Chem. Soc.*, 1980, **102**, 7211–7218.

22 F. Weinhold and C. R. Landis, *Chem. Educ. Res. Pract.*, 2001, **2**, 91–104.

23 NBO 7.0, E. D. Glendening, J. K. Badenhoop, A. E. Reed, J. E. Carpenter, J. A. Bohmann, C. M. Morales, P. Karafiloglou, C. R. Landis and F. Weinhold, Theoretical Chemistry Institute, University of Wisconsin, Madison, 2018.

24 G. Knizia, *J. Chem. Theory Comput.*, 2013, **9**, 4834–4843.

25 G. Knizia and J. E. M. N. Klein, *Angew. Chem. Int. Ed.*, 2015, **54**, 5518–5522.

26 G. Knizia, http://www.iboview.org/index.html.